Concentrations of reactive Mn(III)-L and MnO_2 in estuarine and marine waters determined using spectrophotometry and the leuco base, leucoberbelin blue

Matthew R. Jones [a†‡], George W. Luther III [b], Alfonso Mucci [c], Bradley M. Tebo [a]

[a] Division of Environmental and Biomolecular Systems, Oregon Health & Science University, Portland, OR 97239, USA

[b] School of Marine Science and Policy, University of Delaware, Lewes, DE 19958, USA

[c] GEOTOP and Department of Earth and Planetary Sciences, McGill University, Montreal, QC H3A 0E8, Canada

Current address:

[†]POSTECH – Pohang University of Science and Technology, Division of Environmental Science and Engineering, Pohang-si, Gyoungsangbuk-do, 37673, Korea

[‡]corresponding author

Keywords: MnO2; Mn(III)-L; Spectrophotometry; Leucoberbelin Blue (LBB); Seawater; Manganese speciation

Abstract

In terms of its oxidative strength, the MnO_2/Mn^{2+} couple is one of the strongest in the aquatic environment. The intermediate oxidation state, manganese(III), is stabilized by a range of organic ligands (Mn(III)-L) and some of these complexes are also strong oxidants or reductants. Here, we present improved methods for quantifying soluble reactive oxidized manganese(III) and particulate reactive oxidized manganese at ultra-low concentrations; the respective detection limits are 6.7 nM and 7 pM (100-cm spectrophotometric path length) and 260 nM and 2.6 nM (1-cm path length). The methods involve a simple, specific, spectrophotometric technique using a water-soluble leuco base (leucoberbelin blue; LBB). LBB is oxidized by manganese through a hydrogen atom transfer reaction forming a colored complex that is stoichiometrically related to the oxidation state of the manganese, either Mn(III)-L or manganese(III,IV) oxides (MnO_x). At the concentration of LBB used in this study, nitrite may be a minor interference, so we provide concentration ranges over which it interferes and suggest potential strategies to mitigate the interference. Unlike previous methods devised to quantify Mn(III)-L, which use ligand exchange reactions, the LBB oxidation requires an electron and therefore needs to physically contact manganese(III) for inner-sphere electron transfer to occur. The method for measuring soluble Mn(III)-L was evaluated in the laboratory, and LBB was found to be oxidized by an extensive suite of weak Mn(III)-L complexes, as it is by MnO_x, but could not react with or reacted very slowly with strong Mn(III)-L complexes. According to the molecular structures of the Mn(III)-L complexes tested, LBB can also be used to qualitatively assess the binding strength of Mn(III)-L complexes based on metal-chelate structural considerations. The assays for soluble Mn(III)-L (membrane filtered) and particulate manganese oxides (trapped by membrane filters) were applied to the well-oxygenated estuarine waters of the Saguenay Fjord, a major tributary of the Lower St. Lawrence Estuary, and to Western North Atlantic oceanic waters, off the continental shelf, where there is an oxygen minimum zone (< 67% O_2 saturation). The methods applied can be used in the field or onboard ships and provide important new insights into oxidized manganese speciation.

1.0 Introduction

Total dissolved or particulate manganese concentrations are generally relatively straightforward to quantify, such as by inductively coupled plasma-mass spectrometry (ICP-MS). On the other hand, the quantitative determination of manganese redox and organic ligand speciation is more challenging, requiring specialized techniques, such as measuring manganese(II) and manganese(III) using the porphyrin spectrophotometric technique [1,2] or measuring manganese(III) via a ligand exchange reaction coupled to a variety of detection methods [3,4]. What neither total nor specific manganese species concentrations provide is a direct quantifiable link to biogeochemical cycles because these measurements do not assess the oxidizing potential of the available manganese. For example, manganese(III) is considered to be a very strong oxidant of organic contaminants [5] and can oxidatively degrade estrogen via a single electron transfer reaction [6]. The oxidizing capacity of manganese species is based on the number of electrons they accept, and their redox potential, as determined by the relative strength of the manganese(III)-ligand complexes (Mn(III)-L) or the crystallinity and nature of the manganese(IV) species, as well as the materials adsorbed onto the solid manganese(IV) phases.

Leuco bases of triphenyl methane undergo oxidation to their highly colored stable oxidized product through hydride transfer from the tertiary C-H bond [7,8], but triphenyl methane is insoluble in water which limits its use in analysis of aqueous solutions. One leuco base, leucoberbelin blue (LBB; IUPAC name 2-[bis[4-(dimethylamino)phenyl]methyl]benzenesulfonic acid), was synthesized with a sulfonic acid group, allowing it to be water soluble [9]. LBB synthesis was undertaken to quantify MnOOH produced by the oxidation of manganese(II) by dissolved oxygen in water [9]. LBB is sensitive to oxidation by manganese in oxidation states of three or higher [9]. LBB has most often been used to quantify or confirm the presence of MnO_x in laboratory cultures [10–12] and, more recently, in a range of environmental systems including humic-rich freshwater flowing into and through a water treatment plant [13], estuarine waters [2,4,14,15], and cave systems [12,16]. Thermodynamic calculations by Luther et al. [17] show that LBB can discriminate oxidized manganese from oxidized iron solids. Reactions that involve LBB are formally hydrogen atom transfer (HAT) reactions that occur via one electron transfer steps as $(R_1R_2R_3)C\text{-}H$ forming the radicals $(R_1R_2R_3)C^{\bullet} + H^{\bullet}$ in the process.

Following development and testing of the LBB techniques to measure Mn(III)-L in the laboratory with a variety of soluble manganese(III) complexes, we applied the methods to estuarine and marine samples. Estuarine samples were collected from the Saguenay Fjord, a deep (maximum depth 270 m) and persistently fully oxygenated tributary of the St. Lawrence Estuary in Canada. Both LBB-reactive dissolved Mn(III)-L ($dMn(III)_{LBB\text{-}r}$) and MnO_2 were measured in these samples; the supporting MnO_2 data having been published previously [4]. As a test of the sensitivity of the method for (sub)nanomolar levels of particulate MnO_2, Western North Atlantic Ocean water samples from beyond the continental shelf were also measured.

2.0 Methods

2.1 Acid cleaning procedures

All plasticware for field and laboratory work was cleaned through sequential washes with 3% micro90 detergent and 2.4 M AR grade HCl and multiple rinses in 18.1 MΩ de-ionized water (DI) between washes. For field samples, the sampling bottles were stored filled with 2.4 M trace metal grade HCl. During field sampling, polysulfone filter units were cleaned through brief multiple rinses of 1.2 M trace metal grade HCl followed by DI. The 47 mm, 0.2 µm, Whatman track etched polycarbonate filters were soaked in 1 M HCl for 1 week before rinsing and storage in DI.

2.2 Analytical equipment

UV-Vis spectrophotometric absorbance measurements of field and laboratory samples were carried out using either a World Precision Incorporated 100-cm liquid wave capillary cell (LWCC), a 1-cm cuvette, or a 1-cm path length dip-probe connected through optical fiber cables to an Ocean Optics USB2000 spectrophotometer with halogen light source (HL-200-FHSA). Measurements in the laboratory were also carried out in 48- or 96-well microtiter plates using a SpectraMax M2 UV-Vis plate reader; the path length for a 48-microtiter plate is 1.4 cm and for a 96-microtiter plate it is 0.6 cm.

2.3 Ancillary analytes

Total dissolved manganese (dMn_T) concentrations in the samples from the Saguenay Fjord were measured using ICP-MS. Following 0.2 µm membrane filtration, small volumes of NH_2OH-HCl were added to 15 mL aliquots of the samples, to a final concentration of 14.7 µM. Samples were stored for 14 days before the addition of 4 µL of 6 M HNO_3 (Optima; Fisher) per 1 mL of sample before long term storage at 4 °C. Prior to analysis on an Agilent 7700 ICP-MS, the samples were diluted ten-fold with 1% HNO_3; the detection limit in DI is 0.15 nM manganese, equivalent to 1.5 nM for the ten-fold diluted samples. The recovery of the National Research Council of Canada certified reference material for trace metals in estuarine water, SLEW-3 (S_P ~ 33 and dMn_T = 29.5 ± 4 nM), was 28.6 ± 2.8 nM. The blank for dMn_T was 0.2 µm membrane filtered DI with additions of NH_2OH-HCl and HNO_3, as per the samples. Applying the strong reductant hydroxylamine prior to the acidification of the sample will result in the reduction of any manganese(III) complexed by labile humic material to manganese(II); this step should minimize the co-precipitation of manganese with humic material when the sample is acidified [2,14].

2.4 LBB Reagent

Leucoberbelin blue (LBB, Sigma) was dissolved in DI to produce a 97.4 mM (4% w/v) stock solution and this solution was adjusted to pH 10.5 by adding either a small volume of NH_4OH (20-22% Sigma, final concentration 26 mM) or NaOH. Previous laboratory work indicated that this stock solution is stable, in the dark at 4 °C, for at least 1 year. The precipitate that forms during refrigeration must be re-dissolved by warming the solution to room temperature. For the LBB primary reagent, the stock solution is diluted 100-fold to 974 µM (0.04% w/v LBB) in 175 mM (1%) acetic acid (trace metal grade, Fisher).

2.5 LBB Standardization

The dark blue color (absorbance maximum at 624 nm; Fig. 1) of oxidized LBB is calibrated using $KMnO_4$ standards. $KMnO_4$ standards are prepared gravimetrically with a high degree of precision. In contrast, Mn(III)-L and MnO_x solutions require standardization prior to use, or, if the concentration is high enough, a known molar absorptivity in the standard medium is required. Manganese in $KMnO_4$ is in the +7 oxidation state, so its reduction to manganese(II) stoichiometrically oxidizes 5 LBB molecules [18,19]. $KMnO_4$ calibration curves are corrected

based on the oxidizing equivalents of the manganese, with particulate manganese (pMn) in environmental samples assumed to be MnO_2 (Fig. 1) and the reactive soluble manganese being manganese(III), as manganese(II) does not react with LBB. Calibrations are non-linear: The degree of non-linearity for a 1-cm path length is low and a linear calibration can be used (linear range from 0.05 to > 2 absorbance units), but in a 100-cm LWCC, a quadratic fit to the calibration is required. Under laboratory conditions (in the light and at room temperature), oxidized LBB in DI or seawater is stable for more than 1 week. During field analyses, standards were matrix matched using an aged sample. The presence of interfering ions (Section 3.2, $dMn(III)_{LBB\text{-}r}$ interference) may affect the final absorbance value of these standards, but this can be corrected for by preparing a fresh blank at the time of sample analysis. The detection limit (DL) for the LBB assay is calculated from the standard deviation of a repeated low concentration standard, rather than the blank, because the final concentration of LBB (77.6 μM, 0.0032% w/v) and acetic acid in DI does not affect the absorbance of DI when measured in a 1-cm cell, but does in the 100-cm LWCC.

2.6 Measurement of standards, water samples, and culture media

For the measurement of dissolved LBB-reactive manganese(III) species ($dMn(III)_{LBB\text{-}r}$) in an aqueous sample, the LBB primary reagent is added directly to the sample to a final concentration between 19 (0.0008% w/v) and 78 μM (0.0032% w/v); the former concentration has a lower blank in a LWCC. Adding LBB directly to the sample contrasts with the preparation of the standard solution (see below). The oxidation of LBB is sensitive to the sample matrix (Fig. 2) and variations in the final pH; for these reasons we recommend that the standards for manganese(III) quantification closely matrix match the sample. Accordingly, standard solutions prepared in seawater and estuarine water use a 0.2 μm filtrate sourced from an anticipated low manganese sample (location and water column depth based on previously measured soluble manganese concentrations); the filtrates are aerated for 24 h and re-filtered (0.2 μm) before use. In addition, seawater, culture media, and HEPES (and probably other commonly used buffers) contain material that is oxidized by $KMnO_4$. Therefore, the LBB reagent is added first (in contrast to the procedure for samples) and, after an equilibration period, incremental small-volume additions of $KMnO_4$ and DI are carried out as required. When $KMnO_4$ is added to either DI or seawater after LBB equilibration, these standards, when measured in a 100-cm LWCC,

show a similar absorbance (Fig. 1). In addition, the measurement of seawater samples in a 100-cm LWCC requires that the spectral properties of the standard and sample be similar to minimize the Schlieren effect (i.e., light distortions). Finally, as the presence of, for example, colored dissolved organic material in samples may affect the absorbance in the 100-cm LWCC, a baseline correction on the absorbance measured at 624 nm is calculated. The corrections contain two components: First, all standards and samples are corrected so that the absorbance at 700 nm = 0.000 and then the second correction is applied, which is based on the slope of the linear regression between the absorbance at 480 and 700 nm (Fig. 1). Typically, the DL for manganese(III) in a 1-cm cell is 260 nM and 6.7 nM in a 100-cm LWCC.

2.6.1 Protocol and considerations for $dMn(III)_{LBB\text{-}r}$ field samples

The field procedure applied to the Saguenay Fjord samples ran as follows. Immediately following 0.2 µm membrane filtration, 4.9 mL of the sample was pipetted into a 5 mL polypropylene snap cap tube followed by 0.1 mL of LBB working reagent (final LBB concentration 19.5 µM and 3.5 mM acetic acid). This sample was shaken and left to stand for 3–4 h. As Figure 3C shows, weak Mn(III)-L complexes will react within 20 min, so a 3–4 h time window is sufficient to enable the reaction to run to completion. The reaction time to completion for the oxidation of LBB by NO_2^-, when LBB concentrations are 2–4 times greater than those used, is on the order of 9–12 h (Fig. 4B). The time to analysis, therefore, provides a compromise that limits potential interference by NO_2^- but allows for the manganese(III) reaction to complete.

For practical reasons in estuarine sampling, a matrix match cannot be readily applied between all samples and the calibration (unless undertaking standard additions). Thus, standards were made up in a single media collected from the St. Lawrence Estuary (48°42.06'N 68°39.03'W) at a depth of 50 m and S_P = 32. In a 100-cm LWCC, the light distortion from DI to 0.6 M NaCl (combusted), which is commonly used as the blank to allow for an inter-comparison of marine dissolved organic material, results in a baseline drop of ~0.016 absorbance units at 700 nm; 0.6 M NaCl has an absorbance maximum (~0.04) at 515 nm. The absorbance spectra of the standards and each sample were adjusted as detailed in Section 2.6 to compensate for the presence of organic material. These adjustments also minimized the effect of the light distortion across the salinity gradient, which for these samples ranged from S_P = 3.5 to S_P = 31. An

approximation of this error can be calculated by comparing calibrations in saline and freshwater media (Fig. 1C), the linear component of the slopes of those calibrations, 0.013 and 0.012, respectively, decreases by 0.001. When using a seawater calibration for a freshwater sample, this decrease across the effective analytical range of the 100-cm LWCC (0-240 nM manganese(III); 240 nM approximately equal to 1.8 absorbance units) results in an underestimation of the samples concentration by 8% at 240 nM. As manganese(III) concentrations decrease and/or salinity increases, this error decreases. As well as salinity, the pH of a sample may change across an estuarine gradient and with depth; the addition of acetic acid within the LBB working reagent buffers the pH of the mixed sample. The final concentration of acetic acid is 3.5 mM, which decreases the sample pH_{NBS} to 4.65 ± 0.05. This is in contrast to the 13.9 mM acetic acid solution used during MnO_2 analysis; which decreases the sample pH_{NBS} to 3.67.

2.7 Measurement of the particulate phase retained on filters

The LBB filter-reagent is a dilution of the LBB primary reagent in DI usually to a final concentration of 78 μM (0.0032% w/v). Following collection of the particulate phase, the membrane filters are not rinsed as we do not expect residual sea salts to significantly affect the spectral properties of the sample if measured in a LWCC. Accordingly, filters are immediately placed in polypropylene snap-cap tubes to which 2 or 4 mL of the LBB filter-reagent is added and the sample is shaken. If, after one hour, the coloration of the solution appears saturated, more filter-reagent can be added. Samples are periodically shaken before analysis, in duplicate or triplicate, 4-12 h later. Upon baseline correction, as described above for analyses in a LWCC, the average residual standard deviation (RSD) of duplicate MnO_2 samples, based on measurements of samples retrieved from North Atlantic waters (Section 3.4.2, MnO_2 in offshore North Atlantic water), is 3.2%. The standards for particulate MnO_x are made using $KMnO_4$ in DI. The concentration of MnO_2 calculated following the LBB assay should be similar to that following hydroxylamine extraction of the sample assuming that all of the manganese extracted from the sample is MnO_2 [18]. The DL for MnO_2 (determined based on the $KMnO_4$ standards) in a 1-cm cell is 130 nM and 2.2 nM in a 100-cm LWCC. As particulate MnO_2 is concentrated through filtration, the DL is lowered in proportion to the volume filtered. For the Saguenay Fjord samples, we filtered 275 mL of seawater and added 2 mL of LBB reagent to each filter, the concentration factor of 138 resulted in a DL of 0.02 nM. For the offshore samples, we filtered

625 mL of seawater and added 2 mL of LBB; the concentrating factor was 375 and the effective DL was 0.007 nM.

2.8 Collection of field samples

In September 2014, samples were collected in the Saguenay Fjord from two casts (Stations SAG05 and SAG30) and along a surface water transect (Supporting material (SM) Fig. SM1 and Table SM3). In August 2014, samples were collected from two stations (Stations A1 and A2) during the profiling of an offshore oceanic location (Fig. SM2 and Table SM4). Water samples were collected with a rosette system (12 × 12 L Niskin PVC bottles) equipped with a Conductivity-Temperature-Depth sensor (CTD). Polycarbonate bottles were used to collect the samples from the Niskin bottles by filling the bottles to the brim after rinsing three times with sample water. Samples were stored in the dark at 4 °C and filtered within 30 min through 0.2 μm Whatman Polycarbonate Track etched membrane filters held in polysulfone filtration units. To test for the presence of colloidal MnO_x, some of the 0.2 μm filtrates were immediately filtered through 13 mm, 0.022 μm, polyethersulfone (PES) membrane syringe filters (Tisch Scientific).

3.0 Results

To assess the ability of soluble manganese(III) to oxidize LBB, a suite of Mn(III)-L complexes required synthesis; details of these syntheses are provided in the Supporting material. The oxidation of LBB by solid MnO_2 is well established [9,18,20]; colloidal MnO_2 has also been used to calibrate the LBB technique [15].

3.1 Reaction of LBB with Mn(III)-L complexes

The stoichiometry of the LBB reaction with manganese(III) was established by comparing the absorbance of LBB following its oxidation by either $KMnO_4$, Mn(III)-pyrophosphate (Mn(III)-PP) or manganese(III)-desferrioxamine-B (Mn(III)-DFOB; Fig. 2). Concentrations of the Mn(III)-L stock solutions were ascertained through known molar absorptivities (Supporting material). In these experiments, the $KMnO_4$ and manganese(III) solutions were serially diluted into a 25 mM borax (pH 7.8) solution followed by an addition of LBB to 78 μM (0.0032% w/v), final pH 3.8. Dilutions were made so that the manganese(III) solutions were at 5-times the MnO_4 solution concentration. The measured absorbance resulting from the oxidation of LBB by

253 $KMnO_4$ and Mn(III)-PP were within 1% of each other. Mn(III)-DFOB was unable to oxidize
254 LBB in either the 25 mM borax solution or DI (Fig. 2).

255 Because LBB did not react with Mn(III)-DFOB but did with Mn(III)-PP, the reactivity of LBB
256 with different Mn(III)-L complexes was tested (Mn(III)-L complexes listed in Fig. 3). These
257 complexes were synthesized through the stoichiometric manganous-permanganate reaction, with
258 equi-molar (0.1 M) concentrations of manganese(II) and ligand in DI. All Mn(III)-L solutions,
259 except for manganese(III)-oxalate, which is unstable and was therefore immediately filtered and
260 tested against LBB, were left to stand for 24 h before 0.2 μm membrane filtration prior to testing
261 with LBB. The efficiency of the oxidation of LBB by the Mn(III)-L complexes listed in Figure 3
262 was not quantitatively evaluated, this is because the initial concentrations of the Mn(III)-L
263 solutions were not verified. There are two reasons for not verifying the concentration of
264 manganese(III) in those Mn(III)-L solutions. The first is that some of the Mn(III)-L complexes
265 listed in Figure 3, within the first 24-48 h after synthesis, are unstable. The instability of the
266 complexes over this period is attributed to the complexes producing and reacting with reactive
267 oxygen species during their formation and equilibration [21]. The second reason is that the molar
268 absorptivity coefficient of these Mn(III)-L solutions has not yet been determined. For the
269 Mn(III)-L complexes listed in Figure 3, the absorbance of their solutions after dilution into DI
270 was measured before and 30 min after the addition of LBB to a final concentration of 78 μM
271 (0.0032% w/v; Fig. 3). Significant quantities of oxidized LBB formed in nearly all the Mn(III)-L
272 solutions tested, with the exception of manganese(III)-2,3-dihydroxybenzoic acid,
273 manganese(III)-Tiron and manganese(III)-ethylenediaminetetraacetic acid (EDTA).

274 The kinetics of the reaction between LBB and weak (-oxalate, -formate, -pyruvate and -citrate)
275 and strong (-Tiron, -2,3-dihydroxybenzoic acid and EDTA) manganese(III) complexes were
276 measured in DI. For the weak ligand complexes, the reaction with LBB was complete within 20
277 min, with the exception of manganese(III)-oxalate which was nearing completion (Fig. 3). For
278 the strong ligand complexes, there was a small increase in the absorbance of LBB in the presence
279 of manganese(III)-2,3-dihydroxybenzoic acid and manganese(III)-EDTA but no change in the
280 presence of manganese(III)-Tiron (Fig. 3C). As noted previously, Mn(III)-DFOB (Fig. 2) is non-
281 reactive. The reactivity of LBB towards 20-fold dilutions of the weaker Mn(III)-L complexes in
282 0.35 and 0.7 M NaCl and seawater was also tested. After 30 min, these reactions were complete

283 (data not shown), indicating the usefulness of using LBB to measure soluble Mn(III)-L in higher
284 ionic strength media including seawater. Finally, LBB was used to quantify 100 to 200-fold
285 dilutions of manganese(III)-citrate (4.8 mM), -pyruvate (3.0 mM), -malonate (2.9 mM), and -
286 pyrophosphate (4.2 mM) in aged, 0.2 μm filtered, North Atlantic seawater with an initial salinity
287 of 35. The respective recoveries of Mn(III)-L as $dMn(III)_{LBB\text{-}r}$ ranged between 70 to 105%
288 (Table SM2).

289 ### 3.2 $dMn(III)_{LBB\text{-}r}$ interference

290 LBB can measure solid manganese(IV) and manganese(III); unlike iron, there is little colloidal
291 oxidized manganese (Table 1; Oldham et al. [14]; Stumm and Morgan [22]) so filtration readily
292 separates soluble from particulate manganese phases. MnO_2 capable of passing through 0.2 μm
293 membrane filters has been found in organic(lignin)-rich freshwater environments [23] and
294 enzyme preparations in the laboratory [24], but MnO_2 is unlikely to be present in a 0.2 μm
295 filtrate of high ionic strength, natural waters such as those found in oceanic, coastal and mid- and
296 lower-estuarine environments. On formation, MnO_2 has a negative electrostatic charge which is
297 rapidly neutralized by divalent cations, such as Mg^{2+} and Ca^{2+} that are present in marine waters
298 at millimolar concentrations, resulting in the rapid coagulation and precipitation of MnO_2 [25].
299 Even if colloidal MnO_2 is stabilized in an organic rich-environment, the colloids are vulnerable
300 to loss through flocculation as ionic strength increases [23]. If MnO_2 is formed enzymatically,
301 which occurs on biological surfaces typically larger than the filtrate cut-off, the particulate
302 material is unlikely to pass through the 0.2 μm filter membrane. Aggregation of MnO_x is
303 enhanced at surfaces and this particulate material is also filtered efficiently [26].

304 LBB oxidation by heme (Sigma, bovine) is slow, taking greater than 5 days for a measurable
305 color to develop (data not shown) and if heme were present as a free enzyme, its concentration is
306 unlikely to be significant in natural estuarine and marine waters. Currently, in an oxygenated
307 system, only two other LBB reactants have been found: Cobalt(III) [27] and nitrite (NO_2^-).
308 Cobalt(III) is not likely to interfere in the assay as cobalt seawater concentrations are too low,
309 typically sub-nanomolar [28]. As with all redox reactions, the oxidation of LBB by NO_2^- is a
310 second order reaction dependent on both LBB and NO_2^- concentrations (Fig. 4). The absorbance
311 of seawater containing a minimum of 0.3 μM NO_2^- shows no significant increase at 624 nm after

24 h in a 100-cm LWCC, following an addition of LBB in 1% acetic acid [final concentrations,19.5 μM (0.0008 % w/v) LBB and 3.5 mM acetic acid, pH_{NBS} 4.65; 0.1 mL working reagent to 4.9 mL sample] (Fig. 4A). Seawater, containing a minimum of 1.5 μM NO_2^- shows an increase in its absorbance at 624 nm of 0.073 ± 0.016 after 24 h upon the addition of the same concentration of LBB at the same pH (Fig. 4A). Measuring a sample for Mn(III)-L within 4 h limits the extent of the interference by NO_2^-, as the kinetics of the reaction between LBB and NO_2^- at room temperature is ~36-times slower than with Mn(III)-L, 720 min until full color development (Fig. 4B) compared to ~20 min (Fig. 3). Extrapolating the spectrophotometric measurements from a 100-cm path length to a 1-cm path length, and under the aforementioned conditions, it is unlikely that there is a measurable effect even by 1.5 μM NO_2^-. Increasing the final LBB concentration to 77.9 μM while maintaining the final acetic acid concentration at 3.5 mM (pH_{NBS} 4.65) results in the NO_2^- reaction with LBB increasing the absorbance by 0.224 ± 0.082 absorbance units (100-LWCC, Fig. 4A). Extrapolating this change down to a 1-cm path length cell would translate into a 0.002 absorbance units change, within the analytical uncertainty of the measurements. NO_2^- interference becomes more significant when the pH of the sample is decreased. Adding LBB and acetic acid as *per* the working reagent used during MnO_2 determination [final concentrations, 77.9 μM (0.0032 % w/v) LBB and 13.9 mM acetic acid and a final pH_{NBS} of 3.67; 0.4 mL working reagent added to 4.6 mL sample] lowers the final pH of the mixed sample to less than during the manganese(III) determination. At this lower pH (pH_{NBS} 3.67) but still with 77.9 μM LBB, and for seawater containing 1.5 μM NO_2^-, the absorbance at 624 nm after 24 h in a 100-cm LWCC shows an approximately 4-fold increase relative to the higher pH (pH_{NBS} 4.65) which is used during Mn(III)-L determination (Fig. 4A). The increase in absorbance at the lower pH translates to an increase of 0.008 absorbance units in a 1-cm path length cell.

In suboxic environments, Mn(III)-L and NO_2^- are likely to co-exist, so different strategies can be employed to measure manganese(III) in samples collected under such conditions. The first strategy involves combing three factors, which effectively minimizes this interference. These factors are, decreasing the reaction time to analysis (Figs. 3C & 4B), increasing the final pH from pH_{NBS} 3.6 to 4.6 or higher, and decreasing the LBB concentration from 77.9 to 19.5 μM (Fig. 4A). A second strategy is to calculate the concentration of manganese(III) as the difference

342 in absorbance of a sample with and without an addition of a strong manganese(III) ligand, as
343 strong manganese(III) ligand complexes will not react with LBB (Figs. 2 & 3). The final strategy
344 is to quantify NO_2^- via a separate technique and apply a correction. However, this correction has
345 a large error as the NO_2^- calibration by LBB (Fig. 4A) required to calculate the correction has a
346 large error. Therefore, applying this correction significantly increases the error in the calculation
347 of the manganese(III) concentration. Nevertheless, an accompanying NO_2^- measurement is
348 recommended when using > 20 μM LBB in a 100-cm path length cell.

349 ### 3.3 MnO_x oxidation state

350 The average oxidation state of freshly precipitated MnO_x in oxygenated waters is between 3.7
351 and 4 [29–33]. From an environmental perspective, the assumption that all environmental MnO_x
352 is MnO_2 is debatable but is, nevertheless, a reasonable approximation. Manganese oxidation is
353 mostly mediated by bacterial processes [34] and when coupled with secondary (surface catalyzed)
354 oxide formation [26], the resultant mineral phases contain < 10% manganese(III) unless high
355 (millimolar) concentrations of manganese(II) are present [35]. Given, as noted before, that the
356 LBB assay is unreactive towards manganese(II) [10], for environmental samples where only
357 particulate MnO_x is present, LBB measures the average oxidation state of the manganese(III/IV)
358 oxide [18,19]. Murray et al. [20] found that LBB overestimated the oxidation state of particulate
359 MnO_x, probably due to surface catalyzed air oxidation of LBB, whereas, more recently, Zhu et al.
360 [18] found an exact stoichiometric match. Based on the LBB oxidation stoichiometry, if MnO_x
361 contains 10% manganese(III) it introduces an error of –5% in the measurement of MnO_2
362 concentrations; thus, assuming that LBB-reactive pMn is MnO_2 is a reasonable assumption for
363 most samples.

364 ### 3.4 Field Results

365 The LBB technique devised for soluble and particulate phases was applied to estuarine and
366 marine waters and used different filtration cutoffs to ensure the 0.2 μm filtrate is dissolved
367 Mn(III)-L. Estuarine samples were collected from the Saguenay Fjord (Fig. SM1) and oceanic
368 samples were collected in the Western North Atlantic off the continental shelf (Fig. SM2). A DL
369 in a 100-cm LWCC for $dMn(III)_{LBB\text{-}r}$ of 6.7 nM is too high for oceanic samples; therefore, these
370 measurements were not carried out.

3.4.1 $dMn(III)_{LBB\text{-}r}$ in the Saguenay Fjord

In the Saguenay Fjord, measurable $dMn(III)_{LBB\text{-}r}$ was generally constrained to upper surface waters < 20 m (Fig. 5 and Table SM5). There was no significant evidence of colloidal (0.022 < colloidal < 0.2 µm; Table 1) manganese capable of LBB oxidation in samples collected from the surface water transect as there was on average a 2% difference between measurements of 0.2 and 0.022 µm membrane filtered samples (Table 2). Throughout the surface water transect (~ 3 m deep; $S_P = 13.2 \pm 1.5$, this salinity range excludes the sample collected at Station SAG05 and from 2 m deep), $dMn(III)_{LBB\text{-}r}$ ranged from 46 to 58 nM and comprised 90-100% of the dMn_T (54–57 nM). At Station SAG05, $dMn(III)_{LBB\text{-}r}$ was only measurable at depths of 2 (90 nM, 0.2 µm filtrate; 87 nM, 0.022 µm filtrate; $S_P = 3.5$) and 5 m (47 nM, 0.2 and 0.022 µm filtrate; $S_P = 14.3$), and these samples contained 45 and 56 nM dMn_T, respectively. At Station SAG30, $dMn(III)_{LBB\text{-}r}$ was measurable in surface waters to a depth of 20 m. While salinity increased with depth from $S_P = 14.2$ (2 m) to $S_P = 28.2$ (20 m), $dMn(III)_{LBB\text{-}r}$ decreased from 52 to 7 nM; $dMn(III)_{LBB\text{-}r}$ was also present (8 nM) in the bottom water (250 m).

3.4.2 MnO_2 in offshore North Atlantic water

The vertical distribution of MnO_2 in offshore Western North Atlantic waters presented in Fig. 6 was the first of two station (Stations A1 and A2) CTD-rosette casts taken three hours apart. Data from the second station are tabulated in the Supplementary material (Table SM6). There is a degree of spatial and temporal difference between these stations, but we found that the reproducibility of the MnO_2 concentrations within samples retrieved from below the euphotic zone was excellent and highlights the accuracy and reproducibility of the method. For samples collected within the euphotic zone, the concentrations of MnO_2 measured in the surface waters (10 m) was 0.88 and 2.15 nM, and at a depth of 97 m, 0.73 to 1.45 nM, the higher concentrations were measured in samples collected during the second cast. In the OMZ, at depths of 195 and 280 m, the average MnO_2 concentration across both casts was 0.73 ± 0.03 nM (4% RSD) and 0.47 ± 0.05 nM (11% RSD), respectively. At 448 m, the deepest repeated sampled depth, was a region with a significant increase in MnO_2 relative to the OMZ; at this depth, the average MnO_2 concentration for the two casts was 2.6 ± 0.4 nM (15% RSD). Only the first cast sampled below a depth of 448 m and, in these deeper samples, MnO_2 concentrations decreased with depth to 0.35 nM in the intermediate waters at 1200 m and increase back to 3.5 nM MnO_2, at 2600 m.

4.0 Discussion

4.1 Reactivity of Mn(III)-L towards LBB

LBB is well-known for its stoichiometric reactivity towards particulate forms of manganese(III,IV) oxides [9,18,20]. Here, we have shown that LBB is oxidized by a range of Mn(III)-L complexes in DI, 0.35 and 0.7 M NaCl, and in seawater (Table 2). The oxidation of LBB by various Mn(III)-L complexes indicates that the chelate binding mode can be used to differentiate between weak and strong complexes. Strong Mn(III)-L complexes include four ligands, DFOB, EDTA, 2,3-dihydroxybenzoic acid, and Tiron, for which there is little or no reaction with LBB. DFOB has 3 hydroxamate binding modes whereas Tiron and 2,3-dihydroxybenzoic acid have at least 2 catecholate binding modes. EDTA has 4 carboxyl and 2 amine groups for binding. These four ligands have binding modes that comprise 5 membered rings, including the manganese(III), that are planar or near planar. Manganese(III) is likely fully bound without an open manganese site for DFOB, EDTA, 2,3-dihydroxybenzoic acid and probably for Tiron (OH^- is likely involved in axial positions). The reaction of LBB with oxidized manganese is an inner sphere process [36] so dissociation of the ligand, without reduction of the manganese(III) by the ligand, must occur. Our reactivity results indicate that there is no significant dissociation of ligands (L) from these strong Mn(III)-L complexes to permit inner sphere electron transfer.

The weak complexes will undergo dissociation of L from Mn(III)-L and are, therefore, reactive towards LBB. Weak organic Mn(III)-L complexes have one carboxyl and one hydroxyl group that form 6-membered rings or 5-membered rings that are not planar with 6-membered complexes being less stable [37]. These carboxyl ligands have smaller stability constant (K) values and dissociate more readily. Similarly, pyrophosphate also forms 6-membered rings that are not planar. Thus, LBB at sample or higher pH permits discrimination of molecular structure between weak or strong Mn(III)-L complexes.

4.2 Reactive Mn(III)-L in estuarine systems

Saguenay Fjord field samples measured for $dMn(III)_{LBB\text{-}r}$ were also measured for Mn(III)-L using two ligand exchange methods [4,14]. The first method used the competitive ligand

exchange of the combined manganese(II) and natural manganese(III) ligand pool with a cadmium substituted porphyrin complex, α,β,γ,δ-tetrakis(4-carboxyphenyl)porphine [1,38,39]. If exchange occurs within 5 min, this dissolved manganese is either manganese(II) or weakly complexed manganese(III). If, following the addition of a reductant to the sample, there is a further formation of the manganese-porphyrin complex, the difference indicates the presence of manganese(III) in strong complexes [2,14,15,39]. This technique was only applied to water column samples (10 m and deeper) from SAG30. As expected, the concentration of $dMn(III)_{LBB\text{-}r}$ was always lower than the porphyrin measurement which includes manganese(II) and weakly complexed manganese(III) [14], indicating that a reactive manganese(III) was present, albeit at a low concentration. The $dMn(III)_{LBB\text{-}r}$ present in the surface waters, comprised 90–100% of the dMn_T, as measured by ICP-MS and following the sampling protocols above.

The second method used the competitive equilibration of the natural manganese(III) ligand pool with the siderophore DFOB ($Mn(III)\text{-}L_{DFOB}$; [4]). Relative to the DFOB method, which has a DL < 0.09 nM, the LBB technique is less sensitive with a DL of 6.7 nM, similar to the DL of the porphyrin technique (3 nM in seawater). Whereas $Mn(III)\text{-}L_{DFOB}$ increased seaward throughout the surface transect and was inversely related to the abundance of MnO_2, suggesting reductive dissolution of MnO_2 as one formation mechanism [2], $dMn(III)_{LBB\text{-}r}$ showed a linearly proportional loss with dilution by seawater (conservative mixing; Fig. SM3). In the Saguenay Fjord, as in most estuaries, terrestrial colored dissolved organic material (CDOM) shows conservative mixing, both vertically and horizontally [40]. That $dMn(III)_{LBB\text{-}r}$ displays a similar behavior, suggests that terrestrially sourced CDOM or a derivative may be important in stabilizing manganese(III) in $dMn(III)_{LBB\text{-}r}$. There is a greater recovery of Mn(III)-L by LBB than by DFOB throughout the surface water transect, 13 to 99-times. Given that the DFOB method is a ligand exchange method, which is time and concentration dependent, whereas the LBB method is an oxidative reaction through hydrogen atom transfer (HAT), the difference in recovery suggests that the ligands stabilizing manganese(III) can form complexes that will undergo HAT. In the shallow waters (< 20 m) of the Saguenay Fjord, these terrestrially sourced ligands would be present at a sufficiently high concentrations to inhibit a significant ligand exchange with DFOB. In the water column of SAG30, so away from the higher concentration of terrestrial ligands, we were unable to compare $dMn(III)_{LBB\text{-}r}$ to $Mn(III)\text{-}L_{DFOB}$ (~ 2.6 nM) as, if $dMn(III)_{LBB\text{-}r}$ was present, it's concentration below the detection limit (6.7 nM).

460 The $dMn(III)_{LBB\text{-}r}$ concentration in the surface sample at SAG05 (2 m, S_P = 3.5, the most
461 landward station) was twice the concentration of dMn_T (45 nM). To account for this apparent
462 anomaly, we propose that the $dMn(III)_{LBB\text{-}r}$ which passed through both 0.2 and 0.022 µm
463 membrane filters at a similar concentration (90 and 87 nM respectively), was most likely
464 nanoparticulate MnO_2 stabilized by a terrestrial, organic-rich matrix. There is a difference in the
465 calibration of LBB due to the oxidizing equivalents of the manganese species. Using the MnO_2
466 calibration (2 oxidizing equivalents) gives the concentration of the sample collected from SAG05
467 2 m as 45 and 44 nM, respectively, *versus* the dMn_T concentration of 45 nM. As noted above,
468 MnO_2 is unlikely to be present in a 0.2 µm filtrate of a higher ionic strength, natural aqueous
469 solution [25,26]. Thus, the low ionic strength, S_P = 3.5, of this sample and the higher
470 concentration of terrestrial organic matter are likely capable of retaining some (nano) particulate
471 MnO_2 in solution. This hypothesis is supported by the subsequent rapid loss of this signal with a
472 small increase in depth (2 to 5 m) but large increase in salinity (3.5 to 14.3), suggesting that the
473 significant increase in ionic strength resulted in a flocculation of the organic matrix, leading to
474 either the reduction of the MnO_2 [41] or its rapid precipitation. Coincidently, over the same
475 depth range, particulate MnO_2 decreased from 20 to 7.5 nM.

476 In the St Lawrence Estuary, where the Saguenay Fjord surface waters flow into the main estuary,
477 NO_2^- concentrations are low (0.25 µM) and decrease with depth to 0.15 µM by 150 m [42].
478 Waters at a depth of 50–150 m in the main estuary are the source waters for deep water in the
479 Saguenay Fjord [43–45], therefore, their NO_2^- concentration should be low. Nevertheless, using
480 the main estuary's deep water as the nearest neighbor example, the bottom waters of the fjord
481 may contain a maximum of 1.7 µM NO_2^- [46]. Within the bottom waters of the fjord, there was
482 no significant concentration of $dMn(III)_{LBB\text{-}r}$.

483 ### 4.3 Ultra-low concentration of reactive MnO_2 in oceanic water

484 The concentrations of MnO_2 on filters from samples taken at the offshore Atlantic Ocean shelf
485 locations are the first direct measurements of solid MnO_2 in offshore marine systems, as opposed
486 to pMn with MnO_x calculated by difference [47] or through acid leaching [48]. Previously
487 reported, at a location to the north-east of the sampling location (Fig. SM2), samples from within
488 the euphotic zone (< 100 m) and trapped on a 0.4 µm membrane filter contained between 0.4–0.8

nM pMn and intermediate waters (200 to 1000 m) contained between 0.2–0.4 nM pMn [49]. In our samples, surface waters (Station A1) contained < 0.9 nM MnO_2 while intermediate waters contained between 0.2–0.4 nM MnO_2, except for those samples affected by the region of MnO_2 production at the lower boundary of the OMZ and elevated MnO_2 in a nepheloid layer. As the concentrations of MnO_2 are similar to those for pMn, we conclude that much of the pMn in these Western North Atlantic waters off the continental shelf is present as MnO_2. This conclusion is in agreement with Lam et al. [47] who estimated that > 70% of pMn is in the form of MnO_x in North Atlantic offshore waters. The elevated MnO_2 at depth, 3.5 nM at 2600 m and 0.5 nM at 2000 m, was likely due to the presence of a nepheloid layer [50] generated by waters flushing through submarine canyons [51]. The presence of nepheloid layers has previously been used to argue for elevated MnO_x concentrations in the deep waters of this region, with MnO_x calculated by difference based on subtracting the expected concentration of manganese, based on its crustal ratio to titanium, from the pMn concentration [47].

5.0 Conclusions

An analytical method was developed that can be used to provide a measure of the oxidative potential of the reactive manganese pool, quantified as the number of electron equivalents of leucoberbelin blue reactive to soluble manganese(III) complexes and MnO_2. The method is specific towards oxidized manganese [17], but, to fully constrain these species, we recommend using the method on both the particulate and soluble phases along with a determination of dMn_T. Higher concentrations of NO_2^- may interfere, but at pH 4.6 and with lower LBB concentrations (~ 20 μM) the reaction of LBB with NO_2^- is slow and this interference is minimized. The LBB technique also provides information on the relative abundance of weak versus strong Mn(III)-L complexes based on metal-chelate structural considerations, which dictate their reactivity. LBB is likely oxidized by manganese(III) in weaker ligand complexes that are part of CDOM and organic matter degradation products, but not by siderophores. In the particulate phase, the LBB measurements likely reflect the true MnO_2 concentration in aquatic systems. This is in contrast to pMn which may not occur solely in oxidized forms [52] or is bound to a recalcitrant terrigenous material [47]. The LBB assay provides a unique quantification of the oxidative ability of the reactive manganese pool, a characteristic which is relevant to better understand the coupled cycling of manganese with nutrients and other elements.

Acknowledgements

This work was supported primarily by research grants from the Chemical Oceanography Program of the National Science Foundation (OCE-1558692 and OCE-1154357 to BMT and OCE-1558738 and OCE-1155385 to GWL) with partial support from the U.S. National Oceanic and Atmospheric Administration Sea Grant program (NA14OAR4170087 to GWL) as well as the National Sciences and Engineering Research Council of Canada (NSERC) through Discovery and Ship-time grants to AM. We are also grateful to the captains and crews of the R/V *Hugh R Sharpe* and R/V *Coriolis II* who made the sampling for this research possible and highly hospitable, as well as Gilles Desmeules for his help in acquiring water samples and Elizabeth Gass for her work on Mn(III)-L synthesis and kinetics with LBB.

Bibliography

[1] A.S. Madison, B.M. Tebo, G.W. Luther, Simultaneous determination of soluble manganese(III), manganese(II) and total manganese in natural (pore)waters, Talanta. 84 (2011) 374–381. doi:10.1016/j.talanta.2011.01.025.

[2] V.E. Oldham, S.M. Owings, M.R. Jones, B.M. Tebo, G.W. Luther, Evidence for the presence of strong Mn(III)-binding ligands in the water column of the Chesapeake Bay, Mar. Chem. 171 (2015) 58–66. doi:10.1016/j.marchem.2015.02.008.

[3] R.E. Trouwborst, B.G. Clement, B.M. Tebo, B.T. Glazer, G.W. Luther, Soluble Mn(III) in suboxic zones, Science. 313 (2006) 1955–1957.

[4] M.R. Jones, V.E. Oldham, G.W. Luther, A. Mucci, B.M. Tebo, Distribution of desferrioxamine-B-extractable soluble manganese(III) and particulate MnO_2 in the St. Lawrence Estuary, Canada, Mar. Chem. 208 (2019) 70–82. doi:10.1016/j.marchem.2018.11.005.

[5] B. Sun, X. Guan, J. Fang, P.G. Tratnyek, Activation of manganese oxidants with bisulfite for enhanced oxidation of organic contaminants: The involvement of Mn(III), Environ. Sci. Technol. 49 (2015) 12414–12421. doi:10.1021/acs.est.5b03111.

[6] X. Wang, J. Yao, S. Wang, X. Pan, R. Xiao, Q. Huang, Z. Wang, R. Qu, Phototransformation of estrogens mediated by Mn(III), not by reactive oxygen species, in the presence of humic acids, Chemosphere. 201 (2018) 224–233. doi:10.1016/j.chemosphere.2018.03.003.

[7] C.D. Ritchie, W.F. Sager, E.S. Lewis, Application of linear free energy relationships to some reactions of triarylmethane derivatives, J. Am. Chem. Soc. 84 (1962) 2349–2356. doi:10.1021/ja00871a016.

[8] N.R. Ayyangar, B.D. Tilak, Basic Dyes, in: K. Venkataraman (Ed.), Chem. Synth. Dyes, Academic Pres, 1971: pp. 103–157.

[9] H.J. Altmann, Bestimmung von in Wasser gelostem Sauerstoff mit Leukoberbelinblau I. Eine schnelle Winkler-Methode, Z Anal Chem. 262 (1972) 97–99. doi:http://aquaticcommons.org/4843/1/68_1972_altm_dete.pdf.

[10] W.E. Krumbein, H.J. Altmann, A new method for the detection and enumeration of manganese oxidizing and reducing microorganisms, Helgoländer Wiss. Meeresunters. 25 (1973) 347–356. doi:10.1007/BF01611203.
[11] F.C. Boogerd, J.P. de Vrind, Manganese oxidation by *Leptothrix discophora*., J. Bacteriol. 169 (1987) 489–494.
[12] E.R. Estes, P.F. Andeer, D. Nordlund, S.D. Wankel, C.M. Hansel, Biogenic manganese oxides as reservoirs of organic carbon and proteins in terrestrial and marine environments, Geobiology. 15 (2017) 158–172. doi:10.1111/gbi.12195.
[13] K.L. Johnson, C.M. McCann, J.-L. Wilkinson, M. Jones, B.M. Tebo, M. West, C. Elgy, C.E. Clarke, C. Gowdy, K.A. Hudson-Edwards, Dissolved Mn(III) in water treatment works: Prevalence and significance, Water Res. 140 (2018) 181–190. doi:10.1016/j.watres.2018.04.038.
[14] V.E. Oldham, A. Mucci, B.M. Tebo, G.W. Luther, Soluble Mn(III)–L complexes are abundant in oxygenated waters and stabilized by humic ligands, Geochim. Cosmochim. Acta. 199 (2017) 238–246. doi:10.1016/j.gca.2016.11.043.
[15] V.E. Oldham, M.T. Miller, L.T. Jensen, G.W. Luther, Revisiting Mn and Fe removal in humic rich estuaries, Geochim. Cosmochim. Acta. 209 (2017) 267–283. doi:10.1016/j.gca.2017.04.001.
[16] M.J. Carmichael, S.K. Carmichael, C.M. Santelli, A. Strom, S.L. Bräuer, Mn(II)-oxidizing bacteria are abundant and environmentally relevant members of ferromanganese deposits in caves of the upper Tennessee River basin, Geomicrobiol. J. 30 (2013) 779–800. doi:10.1080/01490451.2013.769651.
[17] G.W. Luther, A.T. de Chanvalon, V.E. Oldham, E.R. Estes, B.M. Tebo, A.S. Madison, Reduction of manganese oxides: Thermodynamic, kinetic and mechanistic considerations for one- versus two-electron transfer steps, Aquat. Geochem. (2018) 1–21. doi:10.1007/s10498-018-9342-1.
[18] Y. Zhu, X. Liang, H. Zhao, H. Yin, M. Liu, F. Liu, X. Feng, Rapid determination of the Mn average oxidation state of Mn oxides with a novel two-step colorimetric method, Anal. Methods. 9 (2017) 103–109. doi:10.1039/C6AY02472F.
[19] B.M. Tebo, B.G. Clement, G.J. Dick, Biotransformations of Manganese, in: C. Hurst, R. Crawford, J. Garland, D. Lipson, A. Mills, L. Stetzenbach (Eds.), Man. Environ. Microbiol. Third Ed., ASM Press, Washington, DC, 2007: pp. 1223–1238. http://www.asmscience.org/content/book/10.1128/9781555815882.ch100 (accessed October 28, 2018).
[20] J.W. Murray, L.S. Balistrieri, B. Paul, The oxidation state of manganese in marine sediments and ferromanganese nodules, Geochim. Cosmochim. Acta. 48 (1984) 1237–1247. doi:10.1016/0016-7037(84)90058-9.
[21] J.K. Klewicki, J.J. Morgan, Kinetic behavior of Mn(III) complexes of pyrophosphate, EDTA, and citrate, Environ. Sci. Technol. 32 (1998) 2916–2922. doi:10.1021/es980308e.
[22] W. Stumm, J.J. Morgan, Aquatic Chemistry - Chemical Equilibria and Rates in Natural Waters, John Wiley and Son, New York, 1996.
[23] R. Krachler, F. von der Kammer, F. Jirsa, A. Süphandag, R.F. Krachler, C. Plessl, M. Vogt, B.K. Keppler, T. Hofmann, Nanoscale lignin particles as sources of dissolved iron to the ocean, Glob. Biogeochem. Cycles. 26 (2012) GB3024. doi:10.1029/2012GB004294.
[24] C.A. Romano, M. Zhou, Y. Song, V.H. Wysocki, A.C. Dohnalkova, L. Kovarik, L. Paša-Tolić, B.M. Tebo, Biogenic manganese oxide nanoparticle formation by a multimeric multicopper oxidase Mnx, Nat. Commun. 8 (2017) 746. doi:10.1038/s41467-017-00896-8.
[25] J.F. Perez-Benito, E. Brillas, R. Pouplana, Identification of a soluble form of colloidal manganese(IV), Inorg. Chem. 28 (1989) 390–392. doi:10.1021/ic00302a002.
[26] J.J. Morgan, Manganese in Natural Waters and Earth's Crust: Its Availability to Organisms, in: A. Sigel, H. Sigel (Eds.), Manganese Its Role Biol. Process., Marcel Dekker, New York, 2000.
[27] Y. Lee, B.M. Tebo, Cobalt(II) oxidation by the marine manganese(II)-oxidizing Bacillus sp. strain SG-1, Appl. Environ. Microbiol. 60 (1994) 2949–2957.

[28] T.D. Jickells, J.D. Burton, Cobalt, copper, manganese and nickel in the Sargasso Sea, Mar. Chem. 23 (1988) 131–144. doi:10.1016/0304-4203(88)90027-8.
[29] S. Kalhorn, S. Emerson, The oxidation state of manganese in surface sediments of the deep sea, Geochim. Cosmochim. Acta. 48 (1984) 897–902. doi:10.1016/0016-7037(84)90182-0.
[30] G.B. Shimmield, N.B. Price, The behaviour of molybdenum and manganese during early sediment diagenesis — offshore Baja California, Mexico, Mar. Chem. 19 (1986) 261–280. doi:10.1016/0304-4203(86)90027-7.
[31] D.E. Canfield, B. Thamdrup, J.W. Hansen, The anaerobic degradation of organic matter in Danish coastal sediments: Iron reduction, manganese reduction, and sulfate reduction, Geochim. Cosmochim. Acta. 57 (1993) 3867–3883. doi:10.1016/0016-7037(93)90340-3.
[32] C.M.G. van den Berg, J.R. Kramer, Determination of complexing capacities of ligands in natural-waters and conditional stability-constants of the copper-complexes by means of manganese-dioxide, Anal. Chim. Acta. 106 (1979) 113–120.
[33] M. Villalobos, B. Toner, J. Bargar, G. Sposito, Characterization of the manganese oxide produced by *Pseudomonas putida* strain MnB1, Geochim. Cosmochim. Acta. 67 (2003) 2649–2662. doi:10.1016/S0016-7037(03)00217-5.
[34] B.M. Tebo, S. Emerson, Microbial manganese(II) oxidation in the marine environment: a quantitative study, Biogeochemistry. 2 (1986) 149–161. doi:10.1007/BF02180192.
[35] J.R. Bargar, B.M. Tebo, U. Bergmann, S.M. Webb, P. Glatzel, M. Villalobos, Biotic and abiotic products of Mn(II) oxidation by spores of the marine Bacillus sp. strain SG-1, Am. Mineral. 90 (2005) 144–154.
[36] G.W. Luther, The frontier-molecular-orbital theory approach in geochemical processes, in: W. Stumm (Ed.), Aquat. Chem. Kinet., John Wiley & Sons Ltd, New York, 1990: pp. 173–198.
[37] G.W. Luther, Inorganic Chemistry for Geochemistry and Environmental Sciences: Fundamentals and Applications, John Wiley & Sons Ltd, New York, 2016. http://www.wiley.com/WileyCDA/WileyTitle/productCd-1118851374.html (accessed September 22, 2017).
[38] A.S. Madison, B.M. Tebo, A. Mucci, B. Sundby, G.W. Luther, Abundant porewater Mn(III) is a major component of the sedimentary redox system, Science. 341 (2013) 875–878. doi:10.1126/science.1241396.
[39] G.W. Luther, A.S. Madison, A. Mucci, B. Sundby, V.E. Oldham, A kinetic approach to assess the strengths of ligands bound to soluble Mn(III), Mar. Chem. 173 (2015) 93–99. doi:10.1016/j.marchem.2014.09.006.
[40] H. Xie, C. Aubry, S. Bélanger, G. Song, The dynamics of absorption coefficients of CDOM and particles in the St. Lawrence estuarine system: Biogeochemical and physical implications, Mar. Chem. 128–129 (2012) 44–56. doi:10.1016/j.marchem.2011.10.001.
[41] J.W. Stuckey, C. Goodwin, J. Wang, L.A. Kaplan, P. Vidal-Esquivel, T.P. Beebe, D.L. Sparks, Impacts of hydrous manganese oxide on the retention and lability of dissolved organic matter, Geochem. Trans. 19 (2018) 6. doi:10.1186/s12932-018-0051-x.
[42] A. Mucci, M. Levasseur, Y. Gratton, C. Martias, M. Scarratt, D. Gilbert, J.-É. Tremblay, G. Ferreyra, B. Lansard, Tidally-induced variations of pH at the head of the Laurentian Channel., Can. J. Fish. Aquat. Sci. (2017). doi:10.1139/cjfas-2017-0007.
[43] M. Belzile, P.S. Galbraith, D. Bourgault, Water renewals in the Saguenay Fjord, J. Geophys. Res. Oceans. 121 (2016) 638–657. doi:10.1002/2015JC011085.
[44] C. Bélanger, Observation and modelling of a renewal event in the Saguenay Fjord, PhD, Université du Québec à Rimouski, 2003.
[45] L. Delaigue, Inorganic carbon dynamics and CO_2 fluxes in the Saguenay Fjord (Québec, Canada), MSc, McGill University, 2018.
[46] F. Cyr, D. Bourgault, P.S. Galbraith, M. Gosselin, Turbulent nitrate fluxes in the Lower St. Lawrence Estuary, Canada, J. Geophys. Res. Oceans. 120 (2015) 2308–2330. doi:10.1002/2014JC010272.

[47] P.J. Lam, D.C. Ohnemus, M.E. Auro, Size-fractionated major particle composition and concentrations from the US GEOTRACES North Atlantic Zonal Transect, Deep Sea Res. Part II Top. Stud. Oceanogr. 116 (2015) 303–320. doi:10.1016/j.dsr2.2014.11.020.
[48] J.K.B. Bishop, M.Q. Fleisher, Particulate manganese dynamics in Gulf Stream warm-core rings and surrounding waters of the N.W. Atlantic, Geochim. Cosmochim. Acta. 51 (1987) 2807–2825. doi:10.1016/0016-7037(87)90160-8.
[49] B.S. Twining, S. Rauschenberg, P.L. Morton, D.C. Ohnemus, P.J. Lam, Comparison of particulate trace element concentrations in the North Atlantic Ocean as determined with discrete bottle sampling and in situ pumping, Deep Sea Res. Part II Top. Stud. Oceanogr. 116 (2015) 273–282. doi:10.1016/j.dsr2.2014.11.005.
[50] P. Puig, X.D. de Madron, J. Salat, K. Schroeder, J. Martín, A.P. Karageorgis, A. Palanques, F. Roullier, J.L. Lopez-Jurado, M. Emelianov, T. Moutin, L. Houpert, Thick bottom nepheloid layers in the western Mediterranean generated by deep dense shelf water cascading, Prog. Oceanogr. 111 (2013) 1–23. doi:10.1016/j.pocean.2012.10.003.
[51] M. Canals, P. Puig, X.D. de Madron, S. Heussner, A. Palanques, J. Fabres, Flushing submarine canyons, Nature. 444 (2006) 354–357. doi:10.1038/nature05271.
[52] B.M. Tebo, Manganese(II) oxidation in the suboxic zone of the Black Sea, Deep Sea Res. Part Oceanogr. Res. Pap. 38 (1991) S883–S905. doi:10.1016/S0198-0149(10)80015-9.

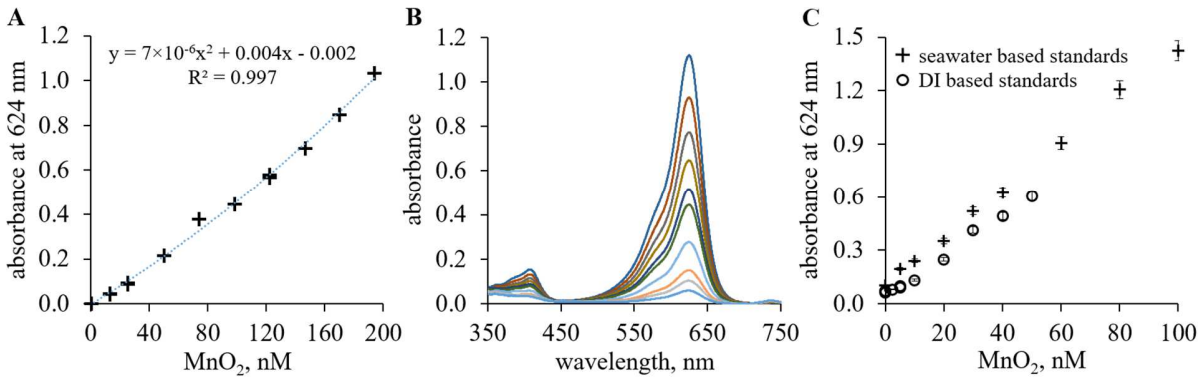

Fig. 1. A, blank and baseline-corrected calibration curve for MnO_2 using $KMnO_4$ as the standard, as measured in a 100-cm liquid wave capillary cell (LWCC); corresponding absorbance spectra of the oxidized LBB standards are shown in B. The standards measured are equivalent to 0†, 12.5‡, 25‡, 49.5, 74, 98.5, 123‡, 147, 170 and 194 nM MnO_2. The blank† was measured in triplicate and select standards‡ measured in duplicate; the absorbance spectra shown for the blank and duplicate standards is the average of those measurements. C, comparison between triplicate measurements of a range of $KMnO_4$ standards produced in seawater and DI, as measured in a 100-cm LWCC. LBB was added to a final concentration of 19 µM (0.0008% w/v) prior to $KMnO_4$.

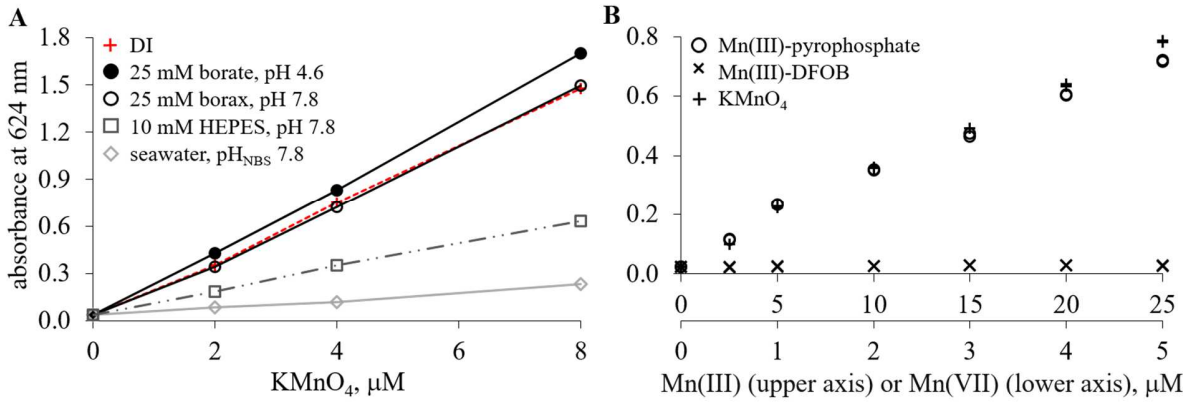

Fig. 2. A, the effect of different aqueous media and pH on the relative absorbance of $KMnO_4$ standards oxidising a final concentration of 78 µM LBB, as measured in 96-well microtiter plates. B, the stoichiometric effect of manganese species on the oxidation of LBB by manganese(III)-pyrophosphate, manganese(III)-deferoxamine-B (DFOB) and potassium permanganate ($KMnO_4$) in 25 mM borax (pH 7.8) measured in 96-well microtiter plates.

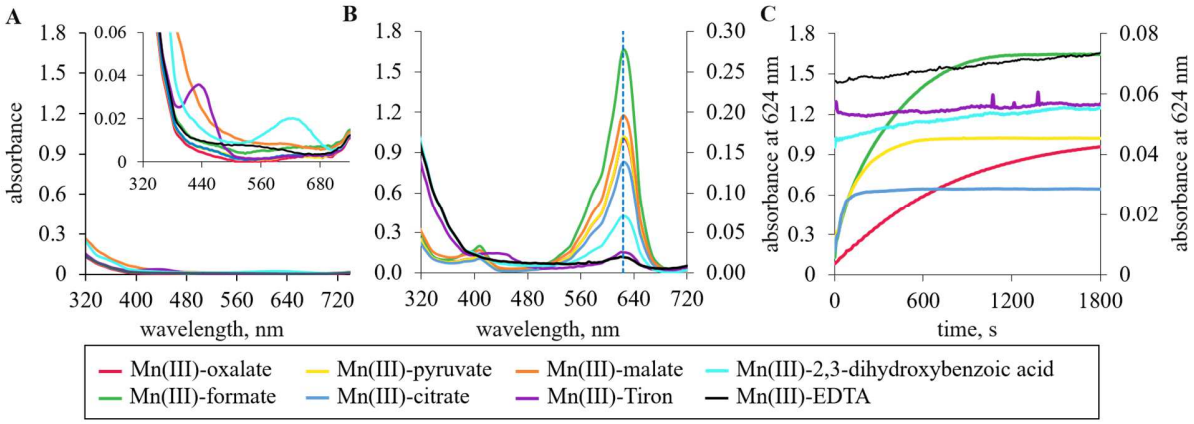

Fig. 3. Absorbance spectra (1-cm cuvette) taken before (A) and 30 min after (B) the addition of LBB to Mn(III)-L solutions in DI. Inset A, x-axis zoomed absorbance spectra. Panel C, rate of LBB oxidation by Mn(III)-L in DI, as measured in a 1-cm cuvette. Panels B and C, right-hand axis is used for the change in absorbance of LBB in the presence of Mn(III)-Tiron, Mn(III)-2,3-dihydroxybenzoic acid and Mn(III)-EDTA.

Table 1. Concentration (nM) of $dMn(III)_{LBB\text{-}r}$ in 0.2 and 0.022 µm membrane filtered surface water samples collected in the Saguenay Fjord. Higher concentrations in the 0.022 µm filtered samples are likely caused through analytical uncertainties; however, the removal of a non-manganese containing colloidal material will also result in a reduction in the background signal so that the final calculated concentration following correction maybe higher.

Station (depth (m))	S_P	0.2 µm filtrate			0.022 µm filtrate			% difference
SAG05 (2m)	3.5	90	±	0.8	87	±	0.8	-3
SAG05 (5m)	14.3	47	±	0.9	47	±	0.9	0
SAG20 (2m)	12.2	54	±	0.9	54	±	0.9	0
SAG25 (2m)	11	58	±	0.9	62	±	0.9	7
SAG30 (3m)	15	52	±	0.9	46	±	0.9	-12
SAG36 (3m)	12.2	54	±	0.9	54	±	0.9	0
SAG42 (2m)	13.5	51	±	0.9	55	±	0.9	8
SAG48 (3m)	14.5	46	±	0.9	51	±	0.9	11

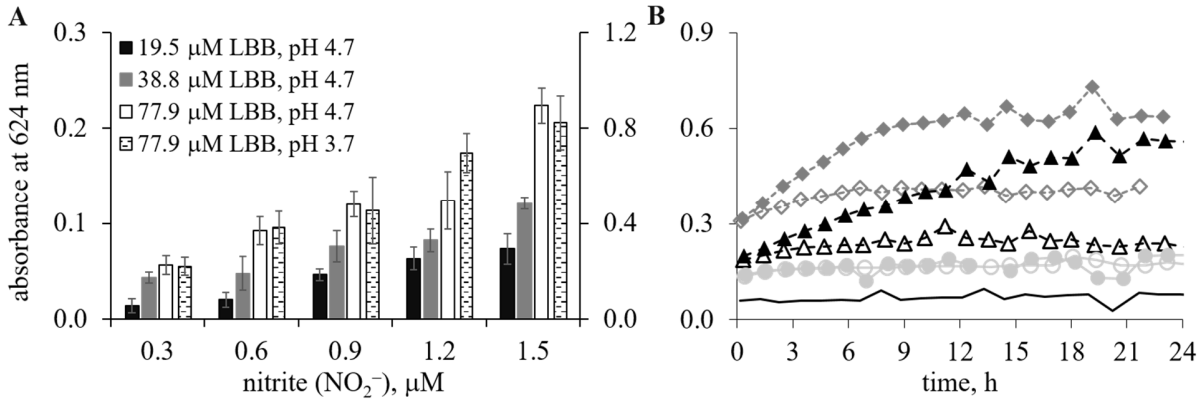

Fig. 4. A, blank corrected increase in absorbance of seawater containing nitrite measured in a 100-cm liquid wave capillary cell (LWCC) at 624 nm, 20 h after an addition of LBB. Errors bars represent standard deviations of triplicate experiments in which each standard was measured in quadruplicate. Left-hand y-axis and solid filled columns, samples measured with a final acetic acid concentration of 3.5 mM (as *per* the $dMn(III)_{LBB\text{-}r}$ protocol). Right-hand y-axis and pattern filled columns, samples measured with a final acetic acid concentration of 13.9 mM (as *per* the MnO_2 protocol). B, kinetics of LBB oxidation during a single experiment measured in a 100-cm LWCC for LBB concentrations of 97.4 (diamonds with dark grey dashed-lines), 45.7 (triangles with black dashed-lines) and 24.4 μM (circles with light grey solid-line) at pH 4.65 (3.5 mM acetic acid in seawater) in the presence of 0.8 μM NO_2^-; filled shapes are the sample with NO_2^- addition, open shapes are without an addition of NO_2^-. The solid black line represents seawater with an addition of acetic acid.

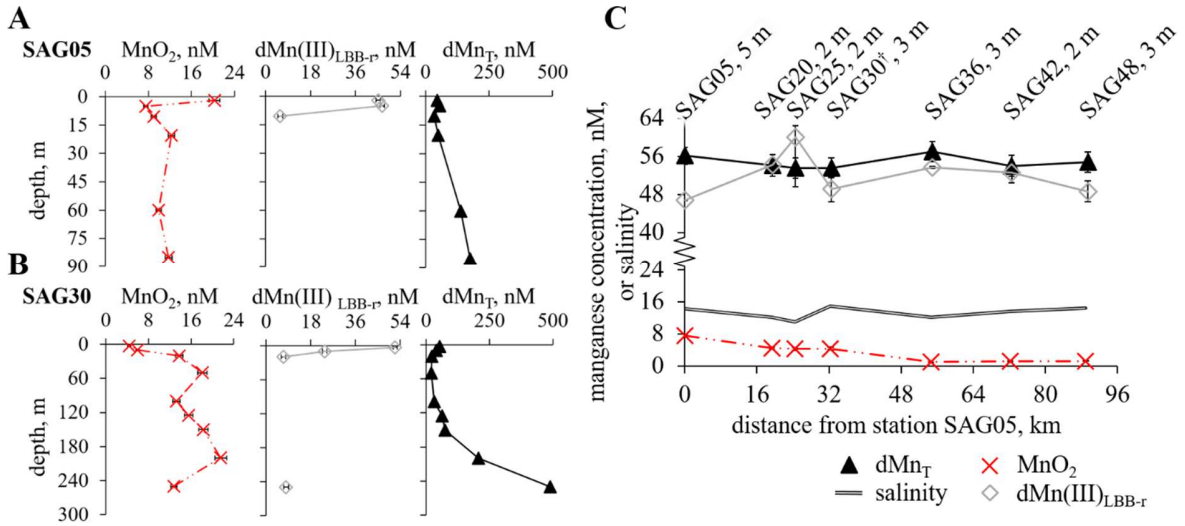

Fig. 5. A and B, depth profiles of manganese species in the Saguenay Fjord; if data points are absent those samples were below the detection limit. The $dMn(III)_{LBB\text{-}r}$ sample at SAG05 and a depth of 2 m we believe to be nanoparticulate MnO_2 stabilized by a terrestrial, organic-rich matrix. C, Concentrations of manganese species and variation in salinity throughout the Saguenay Fjord transect. Station name is represented by SAG## followed by sampling depth in meters. The SAG30† sample was collected 24 h prior to all other samples. Note that the y-axis is compressed between 24-40 nM to allow for better visualization of the data.

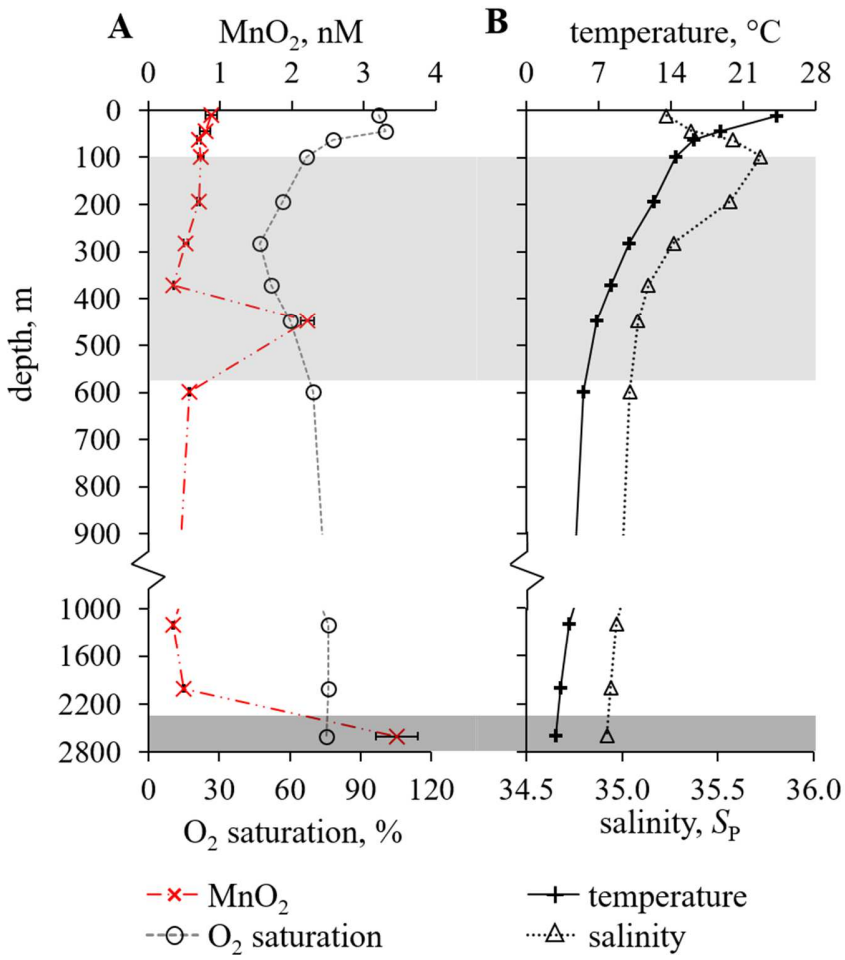

Fig. 6. A, depth profile of O_2 saturation and MnO_2 concentration and, B, temperature and practical salinity in Western North Atlantic water off the continental shelf. The light grey box highlights the OMZ (< 67% O_2 saturation) and the dark grey box the position of samples collected within a likely nepheloid layer. Note that the y-axis is made up of two different scales, 0-900 at 100 m intervals, and 1000-2800 m at 600 m intervals to allow for better visualization of the data

MnO_2
or
MnOOH
or
Mn(III)–L

+

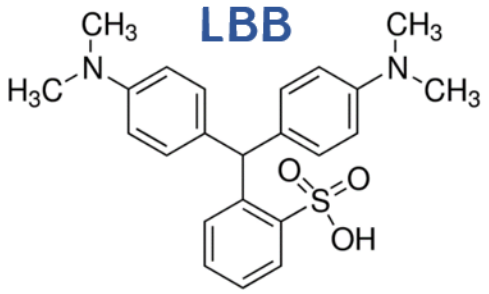

→

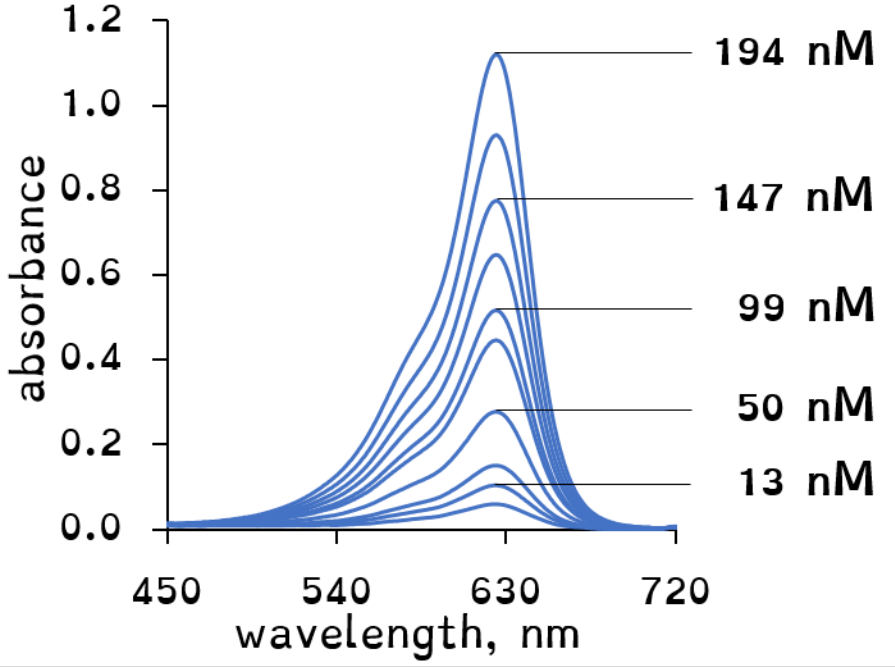

L = { –oxalate –pyruvate –formate –citrate –malate –pyrophosphate

e^-

$M^{m+}(L:) + H\text{–}Y_{LBB} \rightarrow M^{(m-1)+}(LH) + Y_{LBB}$

H^+